Photoelastic Analysis of Partially Occluded Objects With an Integral-Imaging Polariscope

Hector Navarro Fructuoso, Manuel Martínez-Corral, Genaro Saavedra Tortosa, Amparo Pons Marti, and Bahram Javidi, *Fellow, IEEE*

***Abstract*—Polariscopes are the basic instruments used for the analysis of the stress state of transparent materials. Polarized light passing through a 3D object carries the integrated effect of the stress field along the light path. Therefore, conventional polariscopes are not able to discern the stress state of objects involving multiple plates with mutual occlusions. In this paper we propose a novel experimental system for three-dimensional stress analysis based on the combination of a polariscope and Synthetic Aperture Integral Imaging technique. Experimental results show the system's ability to recover the information of the stress distribution of a set of plates located at different depths having mutual occlusions.**

***Index Terms*—Integral imaging (InI), photoelasticity, polariscope.**

I. Introduction

POLARISCOPES have demonstrated to be a powerful tool for the analysis of the stress distribution in transparent materials, but when the object under analysis involves multiple surfaces having mutual occlusions, polariscopes are not able to separate the stress at different depths. The reason is that the fringe pattern observed through the polariscope is the result of the integrated effect of the different surfaces passing through. In order to solve this problem, we propose a new system which combines the principles of a conventional polariscope and Integral Imaging (InI) technique. The validity of our proposal have been verified with the experimental results obtained for the reconstruction of the stress state of a set of plane plates located at different depths having mutual occlusions, as a simple proof of concept. This experiment, however, shows the capability of the proposed system to be applied to a wide variety of complex 3D structures made of a photoelastic material, where the various parts of the structure are occluding each other, provided that there are no total occlusions. We want to emphasize that the system is not only able to measure the stresses of objects with occlusions, it is also capable to determine the depth at which a certain stress is located, allowing to create a 3D map of the stresses of an object with complicated geometry.

InI is a multi-view three-dimensional (3D) imaging technique in which a 3D object can be recorded as a set of 2D images captured from different perspectives. This can be done by using a microlens array or a camera array. InI was initially proposed as a 3D imaging and display system [1]. Research conducted in recent years has been addressed to improve the performance of InI [2]–[17]. Researchers have proposed many 3D applications based on InI [18]–[27], including polarimetric image sensing [28], [29].

The polariscope is the basic instrument used in the photoelastic experiment. Photoelastic analysis is widely used for problems in which stress or strain information is required for extended regions in a material. The method is based in the property exhibited by some transparent isotropic solids, whereby they become optically anisotropic, or birefringent, when subjected to stress. Birefringence is proportional to the principal stress difference at any point on the sample. Therefore, when the sample is placed between crossed polarizers, a fringe pattern reveals the internal stresses. The fringes provide both a qualitative map of stress pattern and a basis for quantitative calculations.

There are some approaches that attempt to relate the integrated retardation pattern to the stress distribution along the light path [30], [31]. Codes based on finite-element method and finite-difference method yield the complete stress state [32]. These methods can be used in problems involving multiple plates with mutual occlusions, but require supplementary information about the boundary and initial conditions in the sample. Sometimes is not possible to obtain this information and these methods are not applicable. To overcome these problems we propose here a new method for the stress analysis based on the combination of a polariscope and the Synthetic Aperture InI technique. The advantage of our method is that it does not require any previous information about the stress distribution in any of the plates. It takes benefit of the inherent capacity of InI to perform tomographical reconstructions of 3D scenes and its natural ability for removing occluding objects.

The paper is organized as follows. In Section II we present the basic theory that is behind the photoelastic analysis. Section III describes the operation of a conventional polariscope. Section IV analyzes the principles for the study of 3D photoelasticity and gives the details of the InI technique. In this

Manuscript received June 11, 2013; revised October 04, 2013; accepted October 15, 2013. Date of publication October 30, 2013; date of current version March 12, 2014. This work was supported in part by the Plan Nacional I+D+I, under Grant DPI2012-32994, Ministerio de Economía y Competitividad (Spain), and by the Generalitat Valenciana under Grant PROMETEO2009-077. The work of H. Navarro Fructuoso was supported by the Generalitat Valencia (VALi+d predoctoral contract).

H. Navarro Fructuoso, M. Martínez-Corral, G. Saavedra Tortosa, and A. Pons are with the Department of Optics, University of Valencia, E-46100 Burjassot, Spain (e-mail: hector.navarro@uv.es; manuel.martinez@uv.es; genaro.saavedra@uv.es; amparo.pons-marti@uv.es).

B. Javidi is with Department of Electrical & Computer Engineering, University of Connecticut, Storrs, CT 06269-1157 USA (e-mail: bahram@engr.uconn.edu).

Color versions of one or more of the figures are available online at http://ieeexplore.ieee.org.

Digital Object Identifier 10.1109/JDT.2013.2287767

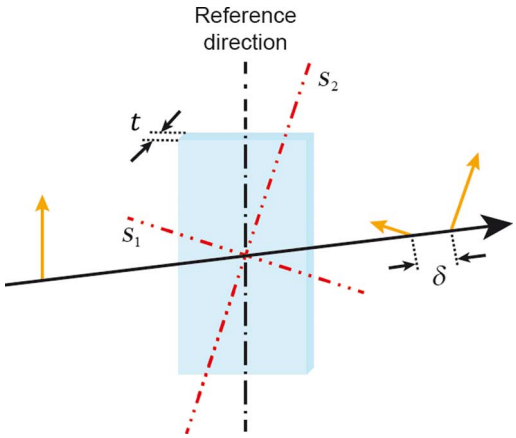

Fig. 1. Linearly polarized light passing through a stressed material. The light separates into two linearly polarized wavefronts traveling at different velocities, each oriented parallel to one of the principal stress directions ($\boldsymbol{s}_1$ and $\boldsymbol{s}_2$). The optical path difference at the output is given by δ.

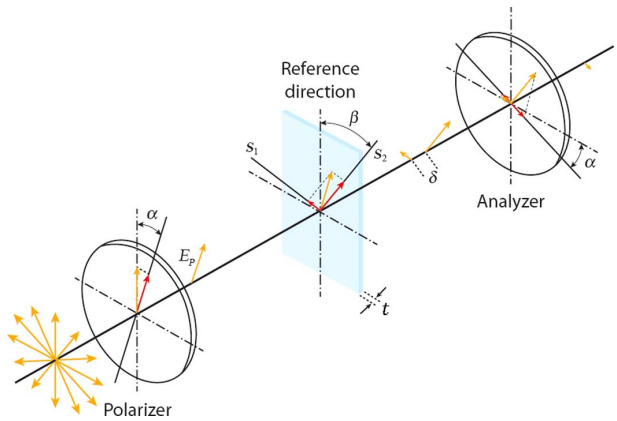

Fig. 2. Plane polariscope. The transmission axes of the linear polarizers are usually crossed. Yellow lines indicate the amplitude and orientation of the electric field of the light waves before reaching each optical element and red lines show the components of the electric field transmitted by each optical element.

section we also explain the set of modifications used to adapt the capture setup of an InI system to build a polariscope for the analysis of partially occluded transparent objects. In Section V we present the reconstruction results for a set of transparent plates located at different depths having mutual occlusions. These results are compared with those obtained by individually analyzing each plate with a conventional polariscope. Finally, in Section VI the main achievements of this paper are summarized.

II. 2D Photoelasticity

As mentioned in the introduction, photoelastic materials behave optically isotropic without stress, but become doubly refractive, or birefringent, when subjected to stress. Let us consider a plate of a photoelastic material whose thickness is small in relation to dimensions in the plane, and the stresses are acting parallel to the plane of the model (see Fig. 1). Under these conditions the material is said to be under plane stress. In such case it is possible to find a Cartesian coordinate system in which the stress tensor has the form[33]

$$\sigma = \begin{pmatrix} \sigma_1 & 0 & 0 \\ 0 & \sigma_2 & 0 \\ 0 & 0 & 0 \end{pmatrix}, \tag{1}$$

where σ_1 and σ_2 are the magnitudes of the principal stresses in the point under consideration. When a linearly polarized lightwave propagates through the stressed material with thickness t, the lightwave is divided into two orthogonal components traveling at different velocities, each linearly polarized and oriented parallel to one of the principal stress directions $\boldsymbol{s}_1$ and $\boldsymbol{s}_2$. The optical path difference between the two beams is given by

$$\delta = qt\,(n_1 - n_2)\,. \tag{2}$$

In this equation, n_1 and n_2 are the refractive indexes experienced by each component along $\boldsymbol{s}_1$ and $\boldsymbol{s}_2$ directions and q is the number of times that the light passes through the material.

The stress-optic law states that the relative change in the refractive index is proportional to the difference between the principal stresses on the material at the point in question. This law can be written as:

$$(n_1 - n_2) = C\,(\sigma_1 - \sigma_2) \tag{3}$$

where the constant C is called stress-optical coefficient and defines a physical property of the material. Combining (2) and (3), we obtain

$$(\sigma_1 - \sigma_2) = \frac{\delta}{qtC}. \tag{4}$$

Based on the above equation, it is possible to obtain the stress difference at any point of the sample from the measurement of the relative retardation if we know the stress-optical constant C of the material under study.

III. Conventional Polariscope

Polariscopes are the basic instruments used for the measurement of the relative retardation in photoelastic experiments. Besides other possible arrangements, polariscopes are generally employed in one of two configurations: the plane polariscope and the circular polariscope. Additionally, polariscopes can work in transmission or reflection modes. For transmission polariscopes, $q = 1$ and for reflection polariscopes, $q = 2$, since in the reflection mode the light must pass twice through photoelastic material.

The plane polariscope consists of a light source and two plates of linear polarizers which usually are crossed. In Fig. 2, we can see a schematic of a plane polariscope.

When the light emitted by a quasi-monochromatic and spatially incoherent source passes through the first polarizer, all components of the light wave are blocked, except those whose direction of vibration coincides with the transmission axis of the polarizer. The linearly polarized light reaches the stressed sample and the electric field is resolved into two components having planes of vibration parallel to the principal stresses. These waves traverse the plate with different velocities and

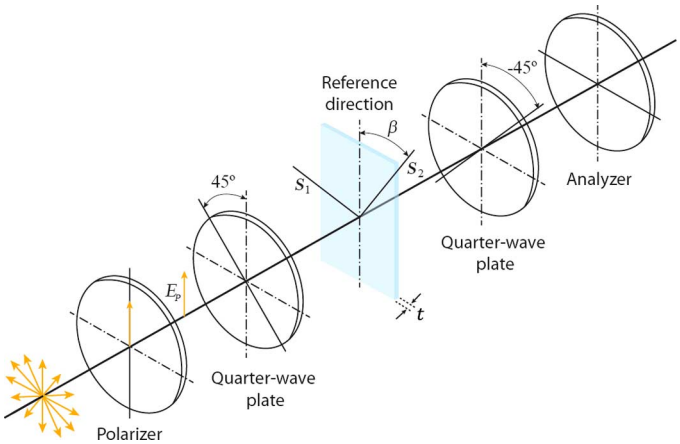

Fig. 3. Usual arrangement for the optical elements in a circular polariscope.

the two waves are no longer in phase when emerging from the sample due to the relative retardation δ. The analyzer will transmit only the projection of the electrical field vector of these two waves onto its principal axis. The resulting light intensity will be a function of the retardation δ and the angle between the analyzer and principal strains $(\beta - \alpha)$. The intensity of the light emerging from the plane polariscope will be

$$I = {E_P}^2 \sin^2 2(\beta - \alpha) \sin^2\left(\frac{\pi\delta}{\lambda}\right) \tag{5}$$

where E_P is the amplitude of the component of the electric field transmitted by the first polarizer and λ is the wavelength of the light emitted by the source.

The circular polariscope, besides using two linear polarizers, also uses two quarter-wave plates which in the common arrangement are usually crossed (see Fig. 3).

In this case the intensity of the emerging light is given by

$$I = {E_P}^2 \sin^2\left(\frac{\pi\delta}{\lambda}\right). \tag{6}$$

In a circular polariscope the intensity becomes zero when

$$\delta = N\lambda,\ \forall N \in \mathbb{N}. \tag{7}$$

A pattern of light and dark bands is formed at the output of the circular polariscope. The fringe order is defined as the value of N. Combining (4) and (7), the principal stress difference can be obtained by

$$(\sigma_1 - \sigma_2) = \frac{N\lambda}{qtC} \tag{8}$$

Comparing (5) and (6), it is easy to see that in essence, the plane polariscope yields the fringe pattern of the circular polariscope, but the intensity of the fringes is modulated by the term $\sin^2 2(\beta - \alpha)$. At any point where the electric field of the incident linearly polarized light is parallel to either local principal stress axis, the wave will pass through the sample unaffected, regardless of wavelength. With crossed polarizers, that light will be absorbed by the analyzer, yielding a black region known as isoclinic band. In order to determine the principal-stress directions throughout the model, the polarizer and the analyzer can be rotated simultaneously. Recording the isoclinic fringes for successive angular positions, a map of the orientations of the principal stresses can be obtained.

Since the delay strongly depends on the wavelength, under white-light illumination, a set of colored fringes will be visible at the output of the analyzer. Thus, each wavelength displays its own fringe pattern and the result is a superposition of patterns for all the wavelengths employed. The locus of points on the sample for which $(\sigma_1 - \sigma_2)$ is constant is known as isochromatic fringes and each such region corresponds to a particular color. In the circular polariscope, only the area in which $\sigma_1 - \sigma_2 = 0$ will appear dark, while in the plane polariscope, the isoclinic pattern appear superimposed to the isochromatic fringes. In practice, for qualitative measurements, the analysis of the isochromatic fringes is performed by visual inspection of the pattern. Color matching is employed, using a separate calibration sample in which color is known as a function of N.

IV. 3D InI Polariscope

The formalism presented in the previous section provides the classical description for the analysis of the stress distribution of 2D models. Some problems involve multiple plates located at different depths and these plates may partially occlude each other. When these scenes are analyzed with a conventional polariscope, polarized light passing through the sample carries the integrated effect of the stress field along the multiple plates passing through. The model behaves like a simple retarder at the point of interest. Hence, we consider a series of retarders along the light path. Each retarder can be represented by the retardation δ and the orientation of the retardation axis β.

In a 2D problem, we only have one plane and it is easy to obtain the retardation and the orientation for each point of the sample from the observed fringe pattern with a conventional polariscope. In a 3D model, the problem is complicated because the orientation and the retardation changes as a function of the plane. One to one correspondence between the fringes observed and the state of a particular point along the light path cannot be established. This problem can be solved by using finite-element methods, but these methods are mathematically intensive and supplementary information is required such as knowing the boundary and initial conditions in the sample.

InI technique, combined with the principles of a conventional polariscope, provides a tool for removing partial occlusions and reconstructs a map of the stresses of a set of plates located at different depths. In the conventional InI the scene is illuminated with a spatially-incoherent light source, and the light reflected or diffused in the surfaces of the different objects composing the 3D scene is collected by a microlens array. An image sensor is conjugated through the microlens array with a central plane of the 3D scene, so that each microlens images a different perspective of the 3D scene onto the image sensor. The use of a microlens array in the capture setup is useful when we want to capture small scenes. If we need to capture large scenes, it is better to use an array of cameras or equivalently the method

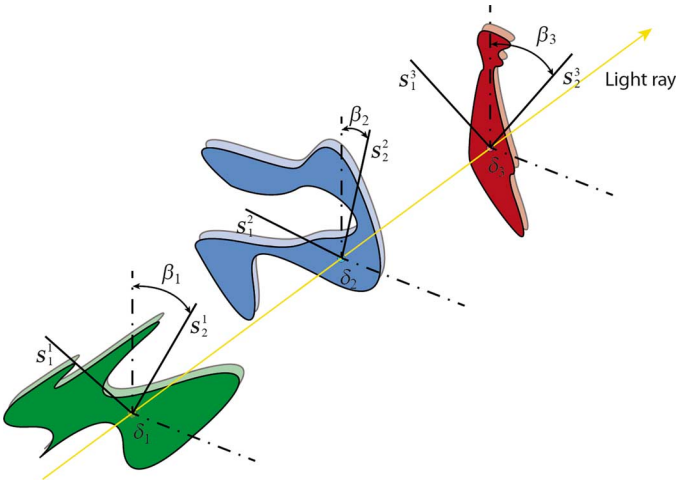

Fig. 4. Polarized light ray passing through a set of three plane plates. Each plate behaves like a simple retarder at the point of interest.

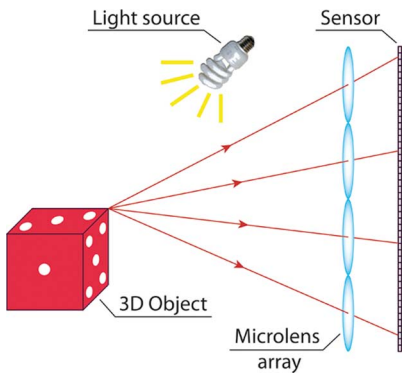

Fig. 5. InI pickup process with a microlens array. The 3D object is illuminated with a spatially-incoherent light source and the light reflected or diffused by the 3D object is collected by each lenslet.

known as Synthetic Aperture Integral Imaging (SAII) [34]. In this method, a digital camera is moved to different positions in order to capture different perspectives of the 3D scene. The advantage of working with SAII is that all the parameters of the capture setup can be modified at will, while by using a microlens array, the period between elemental images, the focal length and the numerical aperture are fixed.

Converting a SAII system into a 3D polariscope requires a series of modifications. In the pickup process, we employ the configuration of the plane polariscope. In Fig. 6, we show a scheme of the proposed system. The light emitted by an array of white light sources is homogenized with a white acrylic diffuser. In front of the diffuser, a linear polarizer selects only the component of the electric field which is parallel to the transmission axis of the polarizing filter. The light that passes through the stressed sample reaches a second linear polarizer whose privileged axis is crossed 90 deg with respect to the first polarizer. This analyzer is mounted in front of the objective of the digital camera. The camera is moved on a rectangular grid over a plane perpendicular to the optical axis in order to capture different perspectives of the light passing through the sample.

We start the analysis of a SAII polariscope with the simplest possible situation. Let us consider a pair of transparent

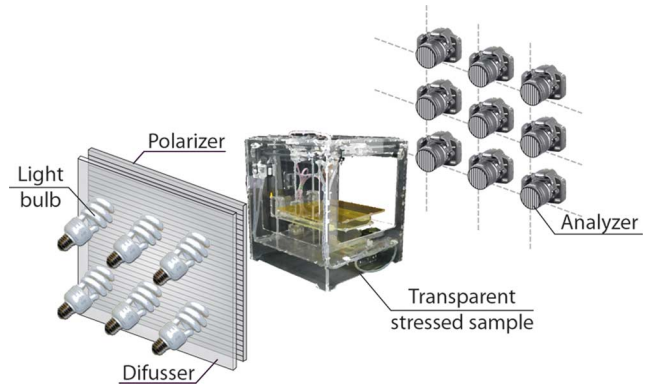

Fig. 6. Scheme of the pickup process with a SAII polariscope.

plane plates under stress located at distances z_1 and z_2 from the camera-lens plane. In the pickup stage, the camera is moved in a rectangular grid with spacing Δ in the (x, y) plane. We assume that the focal length of the camera lens is f and the distance between the lens and the sensor plane is g. For the sake of simplicity, the scheme and also the following equations have been described in the (x, z) plane. The extension to 3D is straightforward.

In Fig. 7, the camera has been modeled by a flat lens and an image sensor located at a distance g from it. According to this model, the polarized light rays passing through the point $P_1\,(x_{P_1}, z_2)$, impact the sensor at

$$x_m = M_{z_2} x_{P_1} + m T_{P_1} \tag{9}$$

where $M_{z_2} = -g/z_2$ is the lateral magnification between the plate and the sensor plane and m is an integer related with the position of the camera on the grid. The pickup period, T_{P_1}, is the distance between replicas in the plane where the camera is moved and is given by

$$T_{P_1} = \left(1 + \frac{g}{z_2}\right) \Delta. \tag{10}$$

If the ray reaching the point x_m only traverses plate 2, the intensity registered in the sensor contains the information of the stress state for that point. However, if the ray also traverses plate 1, the sensor will register the integrated effect of the stresses of the two points of intersection. Light rays passing through the points P_2 and P_3 carry the integrated effect of the stresses on those points, together with the stress on point P_1. When the point P_1 is captured without occlusions, the intensities registered in the sensor for different positions of the camera are identical, while if such point is captured with occlusions, the intensities are different from each other's.

In the reconstruction stage, the back-projection technique described in [19] is used to reconstruct the scene at different depths. In this approach, each captured perspective is computationally back projected onto the reconstruction plane through the center of its associated lens. The back-projected images are summed up to obtain the reconstruction in such plane. After this process, the intensity of non-occluded views is reinforced while the intensities from the occluded views are smoothed by

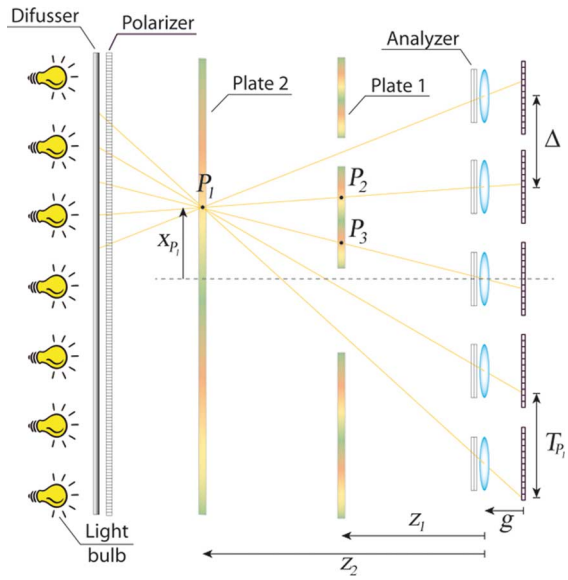

Fig. 7. 2D scheme of the pickup setup with a SAII polariscope. For simplicity the scene is composed by only two transparent plane plates under stress.

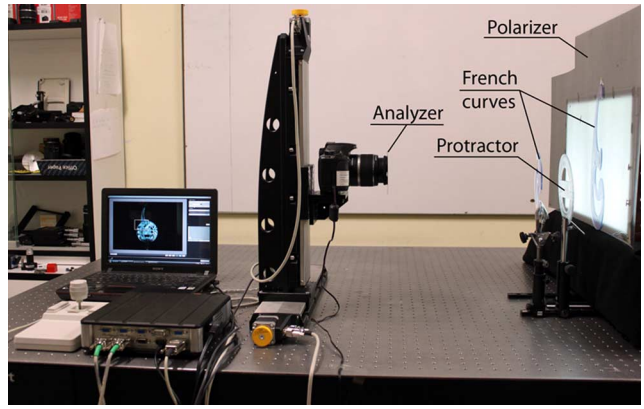

Fig. 8. Experimental setup for the proof-of-concept of the SAII polariscope.

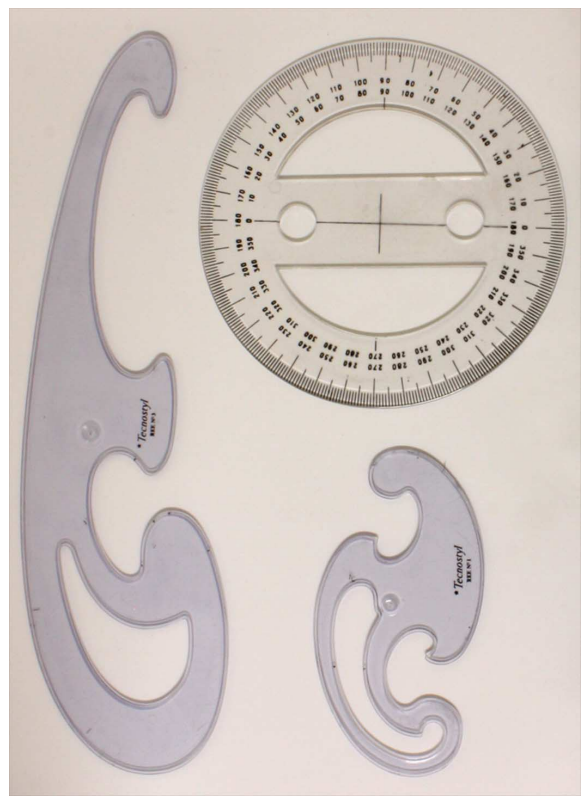

Fig. 9. Drawing tools used in the photoelastic experiment seen under natural illumination.

averaging. Considering the entire 3D scene, if the number of elemental images is large enough, the result of the reconstruction will be the original fringe pattern for the selected reconstruction plane added to a uniform background. Such background may be a problem when it comes to identify the colors of the fringes in the reconstructed image. This problem can be easily solved by filtering the DC term of the Fourier transform of the reconstructed image. This technique may have the drawback of producing contrast reversal in the filtered image. None of the results obtained in this work show this phenomenon, because the average intensity of the image is very low due to the dark areas surrounding the plates. In the case in which the average intensity of the image was high enough, the contrast reversal could occur and this method cannot be used. In that case, other removal methods for partially occluded 3D objects can be applied to this problem in order to enhance the reconstructed image [35]–[38]. The objective of these methods is to identify if the captured pixels belong to an occlusion or to the object of interest. After pixel classification, only pixels which belong to the object are used to reconstruct 3D images at each plane.

V. Experimental Results

The validity of our proposal have been verified with the experimental results obtained for the reconstruction of the stress state of a set of plane plates located at different depths having mutual occlusions.

In the experiment we have implemented the system proposed in Fig. 7. In Fig. 8 we show a picture of the SAII polariscope used in the capture setup. The scene is composed by a protractor and two French curves that are located approximately 330 mm, 380 mm and 440 mm from the camera lens. These drawing tools are manufactured by injecting melted plastic into a mold and differential cooling rates through the thickness of the mold produce residual stresses in the final product. As we can see in Fig. 9, drawing tools used in the experiment are transparent under natural illumination.

The camera is moved over a plane perpendicular to the optical axis in order to capture different perspectives of the light that passes through the samples. A set of 11×11 elemental images was captured by moving the camera in steps of 30 mm on a square grid. Focal length was fixed to 10 mm and the f-number was $f\# = 22$, so that the depth of field of the camera was large enough to capture the whole scene without blurring. The effective camera sensor size is 22.2×14.8 mm and the resolution of the elemental images is 2000×1333 pixels. Fig. 10 shows a subset of views captured with the SAII polariscope.

In Fig. 11, we show the fringe patterns that we would see with a conventional polariscope. Because of occlusions of the

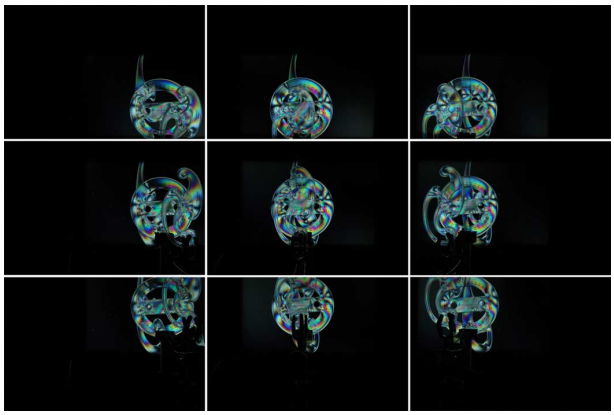

Fig. 10. Set of views corresponding to camera positions: $(5,-5)$, (5,0), (5,5), $(0,-5)$, (0,0), (0,5), $(-5,-5)$, $(-5,0)$ and $(-5,5)$.

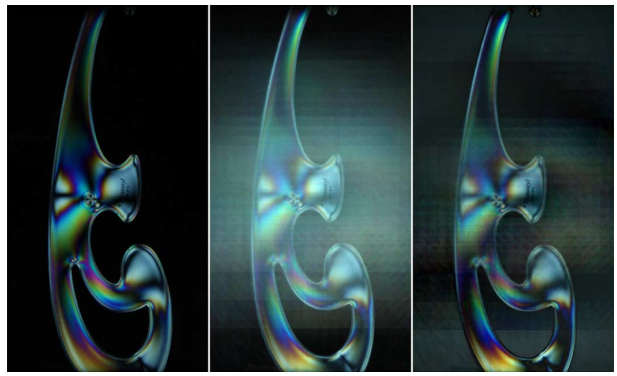

Fig. 12. Fringe pattern captured with a conventional polariscope for the second French curve without occlusions (left image). Reconstruction of the fringe pattern generated by the second French curve captured with the SAII Polariscope having occlusions (central image). Result of filtering the DC term of the reconstructed image in the Fourier domain (right image).

Fig. 11. Set of drawing tools, having mutual occlusions, under the analysis of a conventional 2D polariscope.

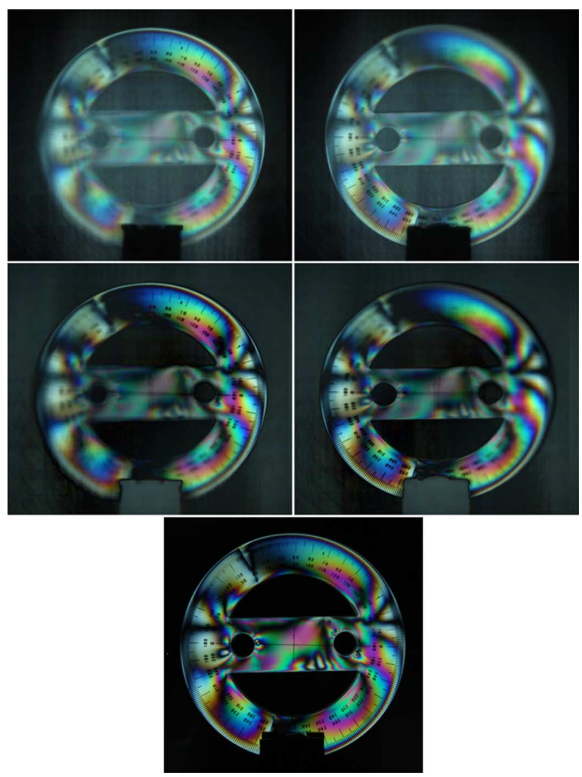

Fig. 13. Reconstructions at two different depths of the fringe patterns captured with the SAII Polariscope for the protractor having occlusions (first row). Same reconstructions after filtering the DC term in the Fourier domain (second row). Fringe pattern captured with a conventional polariscope for the protractor without occlusions (bottom).

multiple objects, this capture does not allow us to relate the stress state of the different drawing tools to the observed fringe pattern.

For distinguishing the fringe patterns corresponding to the plates located at different depths, we apply the reconstruction algorithm described in Section IV to the captured views. To have a reference of the real fringe patterns, we have captured the fringe patterns revealed by each isolated object under a conventional polariscope. The fringe patterns will be compared with those obtained with the SAII Polariscope after applying the reconstruction algorithm for the depths where the drawing tools were located.

The protractor was positioned slightly slanted with respect to the plane perpendicular to the optical axis, so that in the reconstruction stage, some parts appear defocused. This highlights the system's ability to perform tomographic reconstructions at different depths. In Fig. 13, we present two reconstructions at different depths showing this effect. These reconstructions can be compared with the result obtained by individually analyzing the protractor under a conventional polariscope.

In Fig. 14, we show a comparison of the reconstruction for the plane where the first French curve was located (central image) and the same reconstruction after filtering the DC term in the frequency domain (right image). In the left image we can see

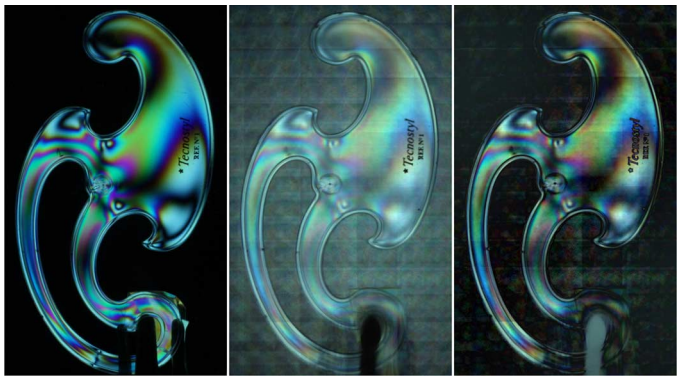

Fig. 14. Fringe pattern captured with a conventional polariscope for the first French curve without occlusions (left image). Reconstruction of the fringe pattern generated by the first French curve captured with the SAII Polariscope having occlusions (central image). Result of filtering the DC term of the reconstructed image in the Fourier domain (right image).

the fringe pattern obtained by individually analyzing this French curve with a conventional polariscope.

VI. Conclusion

In this paper, we have presented a 3D imaging system capable of visualizing the stress state of a set of transparent plane plates having mutual partial occlusions. We captured a set of elemental images containing different perspectives of the fringe patterns revealed by the stressed object after being inserted between crossed polarizers. Tomographical reconstructions for the depths where the different plates where located have been performed. The filtering of the DC term of the reconstructed image allowed us to remove the spurious rays in the reconstructions caused by the mutual occlusions. These reconstructions are compared with the fringe patterns obtained by individually analyzing each plate under a conventional 2D polariscope showing a perfect matching. The proposed procedure permits qualitatively identify the isochromatic regions and the isoclinic bands associated with the magnitude and the orientation of the stress within of each of the plates composing the scene. Note that this would not have been possible with a conventional 2D polariscope. A very interesting application of the proposed system is the realization of a 3D map of the stresses generated within a complex structure, built on a photoelastic material, when subjected to static loads. A conventional polariscope would be unable to obtain this map due to the crosstalk and occlusions between the different sections of the structure. Note that the use of this kind of structures is very common when trying to assess load distributions in large structures by means of down-scaled models having exactly same geometry. Differences between simulations and the real behavior of the loaded structure may be found.

References

[1] G. Lippmann, "Epreuves reversibles donnant la sensation du relief," *J. Phys.*, vol. 7, pp. 821–825, 1908.

[2] H. E. Ives, "Optical properties of a Lippman lenticulated sheet," *J. Opt. Soc. Amer. A*, vol. 21, pp. 171–176, 1931.

[3] C. B. Burckhardt, "Optimum parameters and resolution limitation of Integral Photography," *J. Opt. Soc. Amer.*, vol. 58, pp. 71–76, 1968.

[4] Y. Igarashi, H. Murata, and M. Ueda, "3D display system using a computer generated integral photography," *Jpn. J. Appl. Phys.*, vol. 17, pp. 1683–1684, 1978.

[5] N. Davies, M. McCormick, and L. Yang, "Three-dimensional imaging systems: A new development," *Appl. Opt.*, vol. 27, pp. 4520–4528, 1988.

[6] Okano, H. Hoshino, J. Arai, and I. Yuyama, "Real-time pickup method for a three-dimensional image based on integral photography," *Appl. Opt.*, vol. 36, pp. 1598–1603, 1997.

[7] H. Hoshino, F. Okano, H. Isono, and I. Yuyama, "Analysis of resolution limitation of integral photography," *J. Opt. Soc. Amer. A (Opt., Image Sci. Vision)*, vol. 15, pp. 2059–2065, 1998.

[8] H. Arimoto and B. Javidi, "Integral 3D imaging with digital reconstruction," *Opt. Lett.*, vol. 26, pp. 157–159, 2001.

[9] J.-S. Jang and B. Javidi, "Improved viewing resolution of three-dimensional integral imaging by use of nonstationary micro-optics," *Opt. Lett.*, vol. 27, pp. 324–326, 2002.

[10] S. Jung, J.-H. Park, H. Choi, and B. Lee, "Viewing-angle-enhanced integral three-dimensional imaging along all directions without mechanical movement," *Opt. Express*, vol. 12, pp. 1346–1356, 2003.

[11] R. Martínez-Cuenca, G. Saavedra, M. Martínez-Corral, and B. Javidi, "Enhanced depth of field integral imaging with sensor resolution constraints," *Opt. Express*, vol. 12, pp. 5237–5242, 2004.

[12] Y. Kim, J.-H. Park, S.-W. Min, S. Jung, H. Choi, and B. Lee, "Wide-viewing-angle integral three-dimensional imaging system by curving a screen and a lens array," *Appl. Opt.*, vol. 44, pp. 546–552, 2005.

[13] R. Martínez-Cuenca, H. Navarro, G. Saavedra, B. Javidi, and M. Martinez-Corral, "Enhanced viewing-angle integral imaging by multiple-axis telecentric relay system," *Opt. Express*, vol. 15, pp. 16255–16260, 2007.

[14] B. Javidi, F. Okano, and J. Y. Son, *Three-Dimensional Imaging, Visualization, and Display*. New York: Springer, 2009.

[15] H. Navarro, R. Martínez-Cuenca, A. Molina, M. Martínez-Corral, G. Saavedra, and B. Javidi, "Method to remedy image degradations due to facet braiding in 3D InI monitors," *J. Display Technol.*, vol. 6, no. 10, pp. 404–411, Oct. 2010.

[16] H. Navarro, J. C. Barreiro, G. Saavedra, M. Martínez-Corral, and B. Javidi, "High-resolution far-field integral-imaging camera by double snapshot," *Opt. Express*, vol. 20, pp. 890–895, 2012.

[17] M. Cho and B. Javidi, "Optimization of 3D integral imaging system parameters," *J. Display Technol.*, vol. 8, no. 6, pp. 357–360, Jun. 2012.

[18] M. Pollefeys, R. Koch, M. Vergauwen, A. A. Deknuydt, and L. J. Van Gool, "Three-dimensional scene reconstruction from images," in *Proc. SPIE*, 2000, vol. 3958, p. 215.

[19] S.-H. Hong, J.-S. Jang, and B. Javidi, "Three-dimensional volumetric object reconstruction using computational integral imaging," *Opt. Express*, vol. 12, pp. 483–491, 2004.

[20] S.-H. Hong and B. Javidi, "Three-dimensional visualization of partially occluded objects using integral imaging," *J. Display Technol.*, vol. 1, no. 2, pp. 354–359, Dec. 2005.

[21] A. Stern and B. Javidi, "3D image sensing, visualization, and processing using integral imaging," *Proc. IEEE*, vol. 94, no. 3, pp. 591–608, Mar. 2006.

[22] F. Okano, J. Arai, K. Mitani, and M. Okui, "Real-time integral imaging based on extremely high resolution video system," *Proc. IEEE*, vol. 94, no. 3, pp. 490–501, Mar. 2006.

[23] B. Javidi, S. H. Hong, and O. Matoba, "Multidimensional optical sensor and imaging system," *Appl. Opt.*, vol. 45, pp. 2986–2994, 2006.

[24] J. Arai, F. Okano, M. Kawakita, M. Okui, Y. Haino, M. Yoshimura, M. Furuya, and M. Sato, "Integral three-dimensional television using a 33-megapixel imaging system," *J. Display Technol.*, vol. 6, no. 10, pp. 422–430, Oct. 2010.

[25] Y. Zhao, X. Xiao, M. Cho, and B. Javidi, "Tracking of multiple objects in unknown background using Bayesian estimation in 3D space," *J. Opt. Soc. Amer. A*, vol. 28, pp. 1935–1940, 2011.

[26] A. Yöntem and L. Onural, "Integral imaging using phase-only LCoS spatial light modulators as Fresnel lenslet arrays," *J. Opt. Soc. Amer. A*, vol. 28, pp. 2359–2375, 2011.

[27] R. Horisaki, X. Xiao, J. Tanida, and B. Javidi, "Feasibility study for compressive multi-dimensional integral imaging," *Opt. Express*, vol. 21, pp. 4263–4279, 2013.

[28] O. Matoba and B. Javidi, "Three-dimensional polarimetric integral imaging," *Opt. Lett.*, vol. 29, pp. 2375–2377, 2004.

[29] X. Xiao, B. Javidi, G. Saavedra, and M. E. Martinez-Corral, "Three-dimensional polarimetric computational integral imaging," *Opt. Express*, vol. 20, pp. 15481–15488, 2012.
[30] E. G. Coker and L. N. G. Filon, *A Treatise on Photoelasticity*. London, U.K.: Cambridge Univ. Press, 1931, pp. 143–145.
[31] A. J. Durelli and W. F. Riley, *Introduction to Photomechanics*. Englewood Cliffs, NJ, USA: Prentice-Hall, 1965, pp. 185–186.
[32] H. Mahfuz, T. L. Wong, and R. O. Case, "Hybrid stress analysis using digitized photoelastic data and numerical methods," *Exp. Mech.*, vol. 30, pp. 190–194, 1990.
[33] M. A. Akivis, *Tensor Calculus: With Applications*. Singapore: World Scientific, 2003, pp. 230–236.
[34] S. Jang and B. Javidi, "Three dimensional synthetic aperture integral imaging," *Opt. Lett.*, vol. 27, pp. 1144–1146, 2002.
[35] V. Vaish, M. Levoy, R. Szeliski, C. L. Zitnick, and S. B. Kang, "Reconstructing occluded surfaces using synthetic apertures: Stereo, focus and robust measures," in *2006 IEEE Comput. Soc. Conf. on Comput. Vision and Pattern Recogn.*, 2006, pp. 2331–2338.
[36] D. H. Shin, B. G. Lee, and J. J. Lee, "Occlusion removal method of partially occluded 3D object using sub-image block matching in computational integral imaging," *Opt. Express*, vol. 16, pp. 16294–16304, 2008.
[37] J. J. Lee, B. G. Lee, and H. Yoo, "Image quality enhancement of computational integral imaging reconstruction for partially occluded objects using binary weighting mask on occlusion areas," *Appl. Opt.*, vol. 50, pp. 1889–1893, 2011.
[38] X. Xiao, M. Daneshpanah, and B. Javidi, "Occlusion removal using depth mapping in three-dimensional integral imaging," *J. Display Technol.*, vol. 8, no. 8, pp. 483–490, Aug. 2012.

Hector Navarro Fructuoso (M'10) received the B.Sc. and M.Sc. degrees in physics from the University of Valencia, Spain, in 2008 and 2009, respectively.

Since 2007, he has been with the "3D Imaging and Display Laboratory" at the Optics Department of the University of Valencia. His research interests include focusing properties of light and 3D imaging acquisition and display. He has published 11 articles in major journals and authored 18 communications in prestigious Physics Conferences.

Manuel Martínez-Corral was born in Spain in 1962. He received the M.Sc. and Ph.D. degrees in Physics from the University of Valencia in 1988 and 1993, respectively.

In 1993, the University of Valencia honored him with the Ph.D. Extraordinary Award. He is currently Full Professor of Optics at the University of Valencia, where he is with the "3D Imaging and Display Laboratory". In 2010 he was named Fellow of the SPIE. His research interest includes scalar and vector properties of tightly focused light fields, resolution procedures in 3D scanning microscopy, and 3D imaging and display technologies. He has supervised on these topics six Ph. D. dissertations, two of them honored with the Ph.D. Extraordinary Award, published over seventy technical articles in major journals, and pronounced over twenty invited and five keynote presentations in international meetings.

Dr. Martinez-Corral has been member of the Scientific Committee in over fifteen international meetings, and was the president of the Organizing Committee of the international conference Focus on Microscopy 2007. He is co-chair of the Three-Dimensional Imaging, Visualization, and Display Conference within the SPIE meeting in Defense, Security, and Sensing (Baltimore). He is Topical Editor of the IEEE/OSA JOURNAL OF DISPLAY TECHNOLOGY.

Genaro Saavedra Tortosa received the B.Sc. and Ph.D. degrees in physics from Universitat de València, Spain, in 1990 and 1996, respectively. His Ph. D. work was honored with the Ph.D. Extraordinary Award.

He is currently Full Professor at this University. Since 1999 he has been working with the "3D Imaging and Display Laboratory", at the Optics Department. His current research interests are optical diffraction, integral imaging, 3D high-resolution optical microscopy and phase-space representation of scalar optical fields. He has published on these topics about fifty technical articles in major journals and three chapters in scientific books. He has published over 50 conference proceedings, including 10 invited presentations.

Amparo Pons was born in 1952 in Valencia, Spain. She received the Ph.D. in physics/optics from the University of Valencia in 1987.

She is currently Full Professor of Optics at the University of Valencia where she is with the "3D Imaging and Display Laboratory". Her current research interests include 3D image formation and scanning microscopy, 3D imaging and display technologies and diffractive optics. She is also involved in several physics education projects.

Bahram Javidi (S'83–M'84–SM'96–F'98) received the B.S. degree from the George Washington University, Washington, DC, in 1980, and the M.S. and Ph.D. degrees from the Pennsylvania State University, University Park, PA, USA, in 1982 and 1986, respectively, all in electrical engineering.

He is the Board of Trustees Distinguished Professor at the University of Connecticut, Storrs, CT, USA. He has over 870 publications and has completed 9 books and 54 book chapters. He has published over 380 technical articles in major peer reviewed journals. He has published over 425 conference proceedings, including over 120 Plenary Addresses, Keynote Addresses, and invited conference papers. Some of his journal papers are among the 10 most cited in their topic according to the Thomson Reuters ISI Web of Knowledge. His papers have been cited nearly 11000 times according to the citation index of Thomson Reuters ISI Web of Knowledge ($h\ index\ =\ 55$). He is a coauthor on seven best paper awards.

Dr. Javidi is Fellow of seven professional scientific societies, including the American Institute for Medical and Biological Engineering (AIMBE), the Optical Society of America (OSA), and SPIE. In 2008, he received a Fellow award by John Simon Guggenheim Foundation. In 2010, he was the recipient of The George Washington University's Distinguished Alumni Scholar Award, University's highest honor for its alumni in all disciplines. He received the 2008 IEEE Donald G. Fink prized paper award among all (over 130) IEEE Transactions, Journals, and Magazines. In 2007, The Alexander von Humboldt Foundation awarded Dr. Javidi with Humboldt Prizes for outstanding U.S. scientists. He received the Technology Achievement Award from SPIE in 2008. In 2005, he received the Dennis Gabor Award in Diffractive Wave Technologies by SPIE. He was the recipient of the IEEE LEOS Distinguished Lecturer Award twice in 2003–2004 and 2004–2005. He was awarded the IEEE Best Journal Paper Award from the IEEE Transactions on Vehicular Technology twice in 2002 and 2005. Early in his career, the National Science Foundation named Prof. Javidi a Presidential Young Investigator. In 1987, he received The Engineering Foundation and the IEEE Faculty Initiation Award. He was selected in 2003 as one of the nation's top 160 engineers between the ages of 30–45 by the National Academy of Engineering (NAE) to be an invited speaker at The Frontiers of Engineering Conference which was cosponsored by The Alexander von Humboldt Foundation. He has been an alumnus of the Frontiers of Engineering of The National Academy of Engineering since 2003. He has served on the Editorial Boards of the PROCEEDINGS OF THE IEEE, and the IEEE/OSA JOURNAL OF DISPLAY TECHNOLOGY.